JOURNAL OF MATERIALS SCIENCE 26 (1991) 1056–1060

Grain growth enhancement in silver-doped $YBa_2Cu_3O_{7-x}$ superconductor

G. KOZLOWSKI, S. RELE, D. F. LEE, K. SALAMA
Texas Center for Superconductivity at the University of Houston, Department of Mechanical Engineering, Houston, Texas 77204, USA

The effects of silver addition on the microstructural and superconducting properties of $YBa_2Cu_3O_{7-x}$ (YBCO) have been investigated. It was found that the microstructure of silver-doped YBCO samples is characterized by highly oriented platelet-like grains (up to 3 mm × 0.5 mm × 15 μm). The superconducting transition temperature T_c ($R = 0$) is decreased with increasing wt% of silver. The critical transport density (J_{cT}) is, however, found to be improved (up to two orders of magnitude) in the doped materials (J_{cT} ($T = 77$ K and $H = 0$ T) = 1250 A cm^{-2}). It is believed that the addition of silver lowers the melting temperature of the system and thereby enhances the decomposition of the compound and promotes grain growth during solidification.

1. Introduction

The discovery of high temperature superconductors has generated the exciting possibility of practical applications of these materials at liquid nitrogen temperatures [1]. Most of the applications depend on the ability of the superconducting material to carry sufficiently large amounts of current, i.e., more than 10^5 A cm^{-2} at 77 K in high magnetic fields. Low critical transport current densities (J_{cT}) up to a few hundred A cm^{-2}, typically, have been reported in bulk polycrystalline $YBa_2Cu_3O_{7-x}$ (YBCO) samples. In addition to its poor current-carrying capability, this material is limited by low strength and toughness characteristics. Consequently, novel processing techniques have to be utilized such that the resulting superconductor possesses satisfactory mechanical characteristics while retaining its superconducting properties.

Through the modification of the grain microstructure, both mechanical properties and J_{cT} of YBCO are expected to be altered. It has been demonstrated that directional growth in YBCO material can result in extremely high J_{cT} [2, 3]. It has also been reported recently [4, 5] that significant grain growth is obtained by the partial melting of YBCO doped with Ag_2O. These grains are in the form of stacked platelets with average dimensions of 100 × 50 × 7 μm^3. The directional grain structure observed in these samples can be beneficial in resolving three major problems in the polycrystalline YBCO samples, namely, (1) the presence of weak-link grain boundaries in the path of the supercurrent flow [6], (2) anisotropic superconductivity and (3) anisotropic thermal contraction.

By doping with metallic silver, one can expect to improve the ductility of the superconductor due to the presence of the ductile second-phase constituent [7]. Enhancements in the strength of the material can also result from crack blunting and crack arrest mechanisms which are expected to be active in such a particulate dispersed composite [7]. Long grains of the 1–2–3 phase should form through the formation of a low melting flux, similar to that of the Ag_2O-doped YBCO material. Furthermore, the grain boundary resistance is expected to be lowered, and both the thermal conductivity and the oxygen diffusivity are improved. This paper describes the effects of silver doping in the microstructural and superconducting properties of the YBCO material.

2. Experimental procedure

Samples were prepared by mixing 5, 10, 15, 20, 25 and 30 wt % of silver (99.99 % purity and average particle size of 40 μm) with stoichiometric $YBa_2Cu_3O_{7-x}$ powder commercially available from Grace & Co. (Super Tc-123, average particle size of 20 μm). The powder mixture was ground, uniaxially pressed into pellets 13 mm in diameter and 3 mm thick, and divided into three separate batches. The first batch (6r) was kept at 990 °C for 5 min followed by subsequent cooling at a rate of 60 °C h^{-1} to 960 °C, and then sintered for 24 h at this temperature. The second batch (4d) was cooled from 980 °C at a rate of 4 °C h^{-1} followed by sintering at 940 °C for 24 h. The third batch (6s) was cooled from 990 °C at a rate of 1 °C h^{-1} followed by sintering for 24 h at 960 °C. All samples were held at 600, 500 and 400 °C for 6 h each in the cooling cycle for oxygen uptake. Shrinkage on sintering was approximately 20%, yielding materials with average relative density of 85%.

Resistivity measurements were made on bar shaped samples (~ 10 × 1 × 0.5 mm^3) cut from the sintered pellets using the four-probe method with gold contacts. The temperature was measured by a T-type

0022–2461/90 $03.00 + .12

thermocouple. The measurements of J_{cT} were carried out at $T = 77$ K and $H = 0$ T using a d.c. power supply of 120 A rating (HP model 6011A), and a Keithley 181 nanovoltmeter such that a 1 $\mu V\,cm^{-1}$ voltage criterion is satisfied. The as-sintered surfaces were polished and studied using reflected and polarized light optical microscopy, whereas scanning electron microscopy was used in the study of the fracture surfaces. Electron Probe Microanalysis of the different phases was obtained through a JEOL JXA-8600 electron microprobe equipped with four wavelength dispersive spectrometers (WDS) and an energy dispersive spectrometer (EDS).

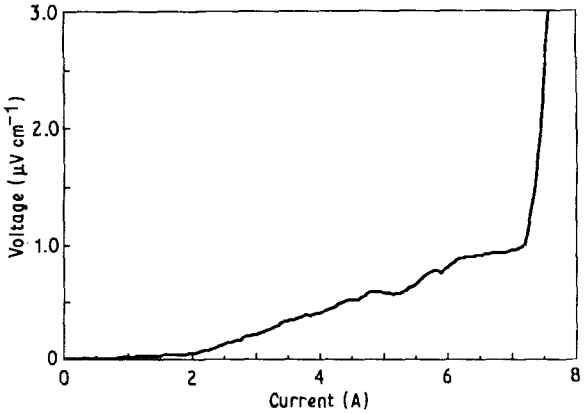

Figure 2 Typical *V–I* curve for a 15 wt % silver-doped YBCO sample (6s).

3. Results and discussion

The resistivity as a function of temperature for the YBCO material doped with silver (4d) is shown in Fig. 1. It is found that increasing amounts of silver lead to a broadening of the transition width concomitant with a decrease in T_c ($R = 0$) from 92 to 84 K. Moreover, it can be seen from Fig. 1 that the resistivity in the normal state of the silver-doped samples drops significantly with silver addition suggesting its presence in the metallic state rather than in its oxide form. This is also supported by the powder X-ray diffraction pattern obtained for these samples, indicating the presence of silver in addition to the Y_2BaCuO_5, $BaCuO_2$ and CuO phases.

Table I summarizes the data which characterize the superconducting properties of the samples used in this work. A typical *V–I* plot for the 15 wt % silver-doped specimen (6s) is shown in Fig. 2. Apart from changes in room-temperature resistivity and critical temperature due to silver doping, Table I indicates the existence of a maximum critical current density at a given silver content within each batch. This improvement in J_{cT} can be explained by the different microstructures of the specimens used in the measurements.

Fig. 3 shows a typical fracture surface of an undoped YBCO specimen (6r). The microstructure of this specimen is characterized by random orientation of monolithic grains with an average grain size of around 40 μm and a minimal amount of liquid phase

TABLE I Superconducting characteristics of the silver-doped YBCO samples.

Ag (wt %)	Room temperature resistivity (4d) (mΩ cm)	T_c (4d) (K)	J_{cT} (6r) ($A\,cm^{-2}$)	(4d) ($A\,cm^{-2}$)	(6s) ($A\,cm^{-2}$)
0	8.6	92	13	20	15
5	5.3	91	27	70	577
10	3.0	93	125	45	203
15	2.1	91	98	11	1250
20	1.3	89	103	6	11
25	0.7	86	175	3	–
30	0.4	84	19	2	–

sintering due to impurities. The fracture surfaces of the 5 wt % silver-doped specimens for all three batches are shown in Fig. 4. From this figure, it is seen that as the cooling rate is decreased, the amount of grain growth is increased and is accompanied by improvements in grain orientation. Fig. 5 shows the effects of varying percentages of silver on the microstructure of the specimens (6r). From the figure, it is found that the development of the oriented platelet-like grains is enhanced as the silver content is increased from

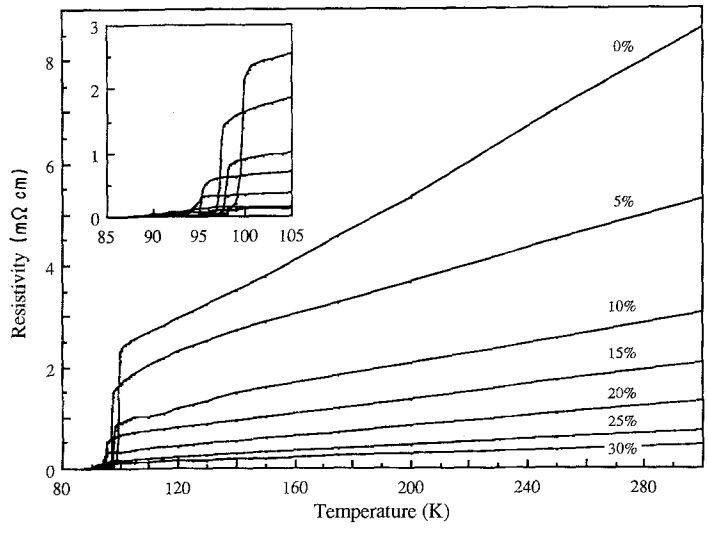

Figure 1 Resistivity as a function of temperature for increasing silver content in silver-doped YBCO specimens (4d).

0 wt % to approximately 20 wt %. Further increase in the silver content results in increasing porosity within the superconductor.

It is apparent from Table I and Figs 4 and 5 that the increase of J_{cT} in the silver-doped YBCO superconductors can be explained by the presence of the long and well aligned grain structure; the maximum J_{cT} values for each batch correspond to the specimens exhibiting the largest and most oriented grains. Reports of the lack of grain growth by metallic silver doping [4] are probably due to non-optimal processing conditions used in manufacturing the specimens [8]. This microstructure of oriented grains is believed to be produced when the YBCO incongruently melts into Y_2BaCuO_5, $BaCuO_2$ and CuO at temperatures above 1014 °C [9] in oxygen. The presence of silver lowers this partial melting and the decomposition temperature. Long, directional and platelet-like grains then slowly nucleate from this melt. The evidence for this decomposition is shown in Fig. 6 where a small amount of $BaCuO_2$ is seen to be trapped by the metallic silver, and the existence of Y_2BaCuO_5 and CuO are indicated. The metallic silver, on the other hand, does not react with any of the decomposed phases as seen from the backscattered image shown in Fig. 6.

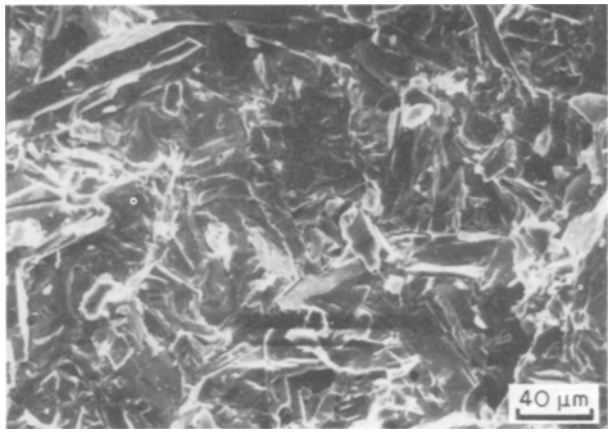

Figure 3 Fracture surface of a 0 wt % silver-doped YBCO superconductor (6r).

Slow cooling seems to play a crucial role in the attainment of the long aligned grains seen in Fig. 4. Fig. 4c shows the microstructure of the oriented platelet-like grains in the form of growth steps. This stepwise microstructure with the smooth facets perpendicular to the length of the grains can be obtained if the growth along the *c*-axis is regulated by the surface nucleation rate [10]. If this is the case, then the long grains will lie in the *a–b* plane. Since the *a–b* plane is considered to be the fast growing plane in the YBCO superconductor, the length of the oriented grains is therefore regulated by the mass transport rate. Consequently, a decrease in the cooling rate will allow additional time for mass transport and nucle-

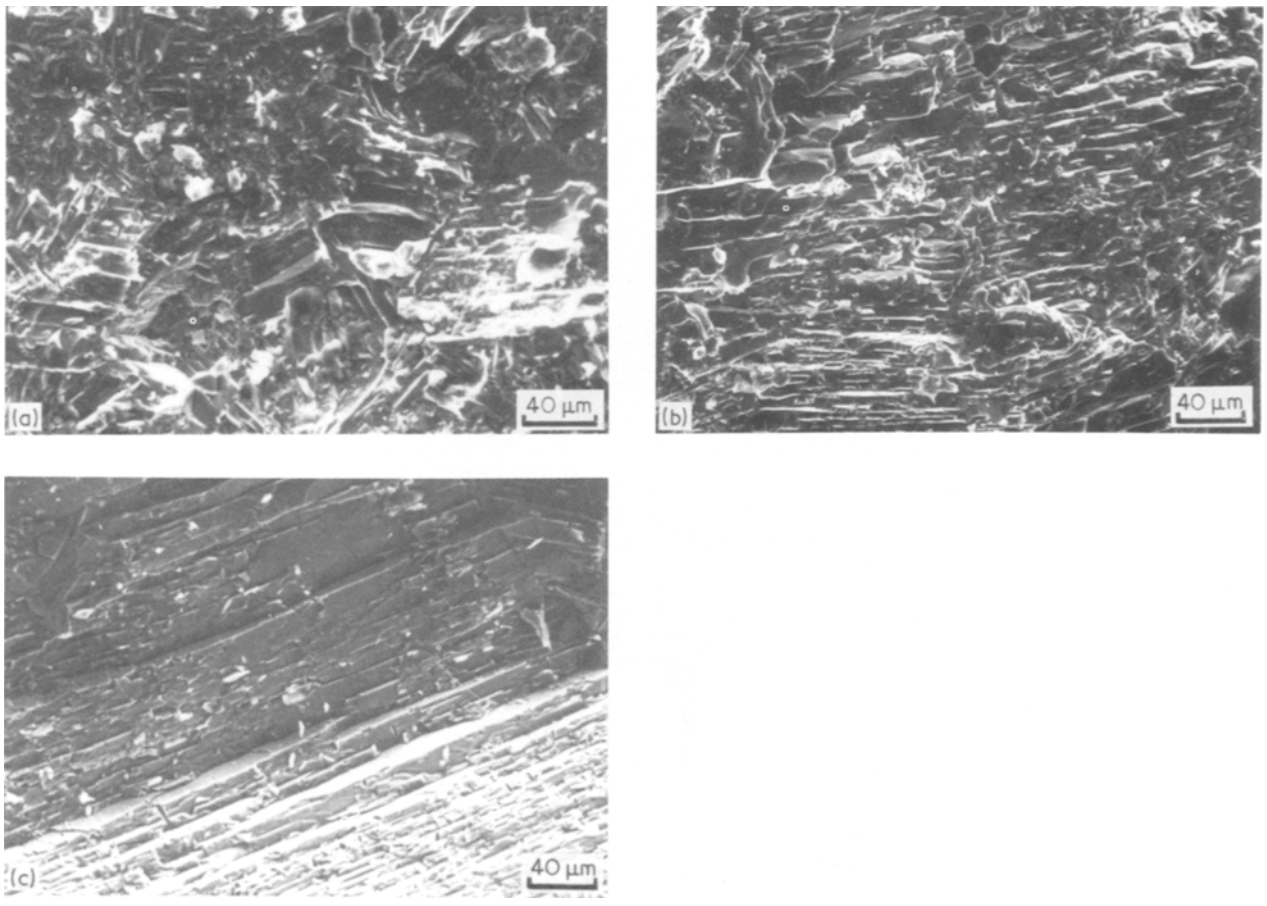

Figure 4 Fracture surfaces of 5 wt % silver-doped YBCO superconductors for batches (a) 6r, (b) 4d and (c) 6s.

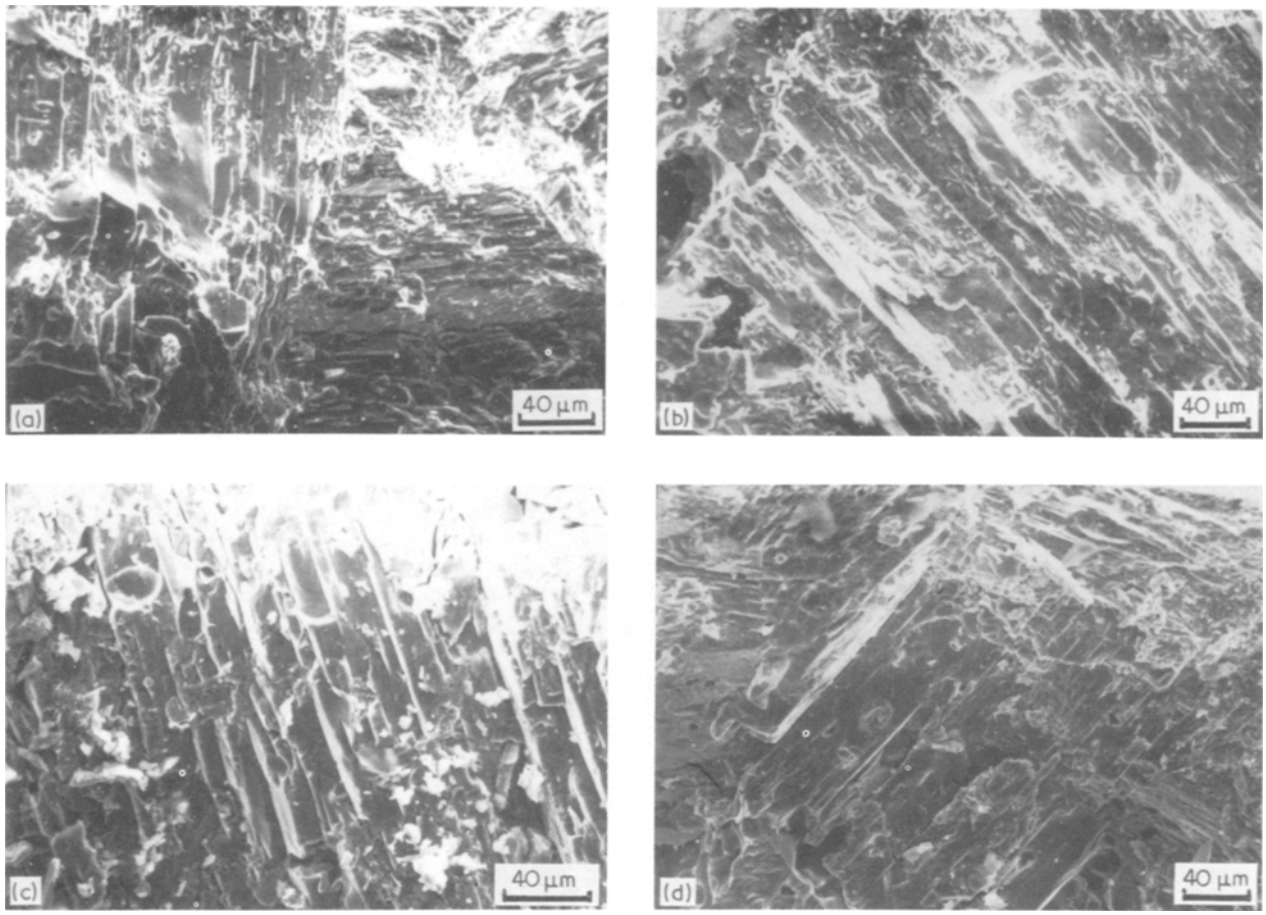

Figure 5 Fracture surfaces of (a) 10 wt %, (b) 15 wt%, (c) 20 wt % and (d) 25 wt % silver-doped YBCO superconductors (6r).

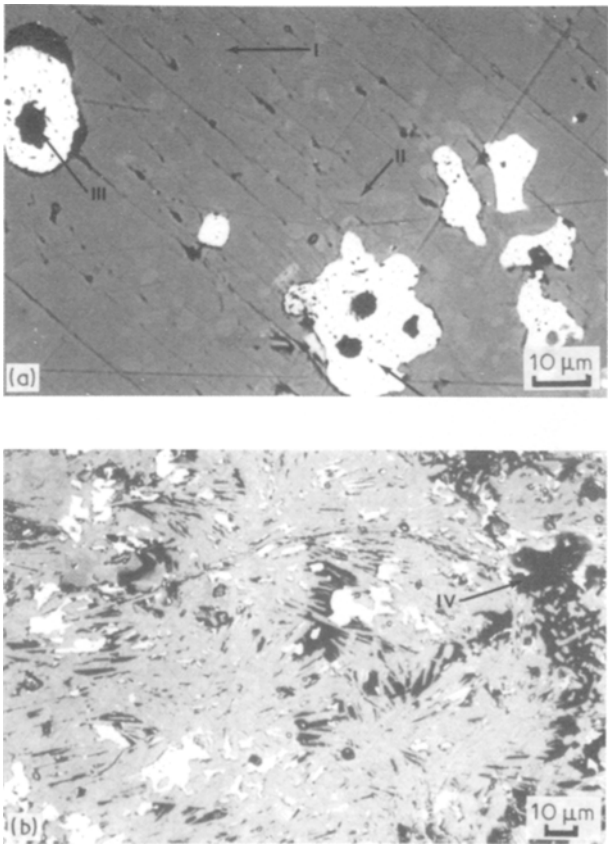

Figure 6 (a) Backscattered image of oriented grains and (b) non-oriented dendritic regions of 15 wt % silver-doped YBCO superconductor (6s) showing [I] $YBa_2Cu_3O_{7-x}$, [II] Y_2BaCuO_5, [III] $BaCuO_2$, [IV] CuO and [V] Ag.

ation to occur, and results in oriented grains over a larger area. The largest of such oriented grains are of the size 3 mm × 0.5 mm × 15 μm and is found in 15 wt % silver-doped YBCO (6s).

The nucleation and growth reaction of the platelet-like structure traps silver between the grains resulting in a lower normal state resistivity for the silver-doped composites as seen in Fig. 1. With increasing amounts of silver (up to 15 to 20 wt %), larger domains of oriented regions are observed. This is because a higher silver content allows a larger amount of YBCO to decompose and undergo the melt-nucleation-growth process. For silver contents in excess of 20 wt %, however, a large amount of mobile melt phases are created which often lead to the egression of some of the molten silver, $BaCuO_2$ and CuO phases from the system. Due to the deficiency of these phases, the recombination reaction cannot proceed to completion, and results in increased porosity (Fig. 5) as well as lower current densities (Table I). The deficiency of barium cuprate and copper oxide is characterized by dendrite-shape and needle-type YBCO phase (Fig. 6) which is seen throughout the samples having higher concentrations of silver. This microstructure is only located on the surface of the samples which have lower silver concentrations. The maximum value of J_{cT} seen around 15 to 20 wt % silver may be shifted to a lower or higher concentration of silver depending on whether the proper amount of elements needed to regain the YBCO phase are present during the resolidification process.

4. Summary

The present study indicates that when silver is added to the YBCO superconductor, it does not react with the decomposed phases but remains in the metallic form. This brings about a lowering of the normal state resistivity of the silver-doped superconductors. Concomitant with this lowering of resistivity are the decrease of transition temperature and the widening of transition width which are due to the increase of the non-superconducting second-phase, i.e., silver. Furthermore, the presence of metallic silver is found to lower the decomposition temperature, and promote a platelet-like morphology of the YBCO grains. By decreasing the cooling rate, sufficient time is allowed for nucleation and mass transport such that the grains are oriented over a larger area. This grain orientation and subsequent growth decreases the amount of Josephson-type weak links, and thereby enhances the transport critical current density of the superconductor. As the amount of silver addition exceeds that of approximately 20 wt %, egression of liquid phases from the bulk material occurs, and recombination to 1–2–3 structure cannot proceed to completion. Consequently, the amounts of porosity and non-superconducting phases are increased, resulting in the lowering of critical transport current density.

Acknowledgements

This work is supported by the Texas Center for Superconductivity at the University of Houston under prime grant MDA 972-88-G-002 to the University of Houston from DARPA and the State of Texas. The authors are grateful to B. Hayman for his kind assistance in the Electron Probe Microanalysis.

References

1. M. K. WU, J. R. ASHBURN, C. J. TORNG, P. H. HOR, R. L. MENG, L. GAO, Z. J. HUANG, Y. Q. WANG and C. W. CHU, *Phys. Rev. Lett.* **58** (1987) 908.
2. K. SALAMA, V. SELVAMANICKAM, L. GAO and K. SUN, *Appl. Phys. Lett.* **54** (1989) 2352.
3. S. JIN, T. H. TIEFEL, R. C. SHERWOOD, M. E. DAVIS, R. B. VAN DOVER, G. W. KAMMLOTT, R. A. FASTNACHT and H. D. KEITH, *ibid.* **52** (1988) 2074.
4. T. H. TIEFEL, S. J. JIN, R. C. SHERWOOD, M. E. DAVIS, G. W. KAMMLOTT, P. K. GALLAGHER, D. W. JOHNSON, Jr, R. A. FASTNACHT and W. W. RHODES, *Mater. Lett.* **7** (1989) 363.
5. C. Y. HUANG, H. H. TAI and M. K. WU, *Mod. Phys. Lett.* **B3** (1989) 525.
6. J. W. EKIN, A. I. BRAGINSKI, A. J. PANSON, M. A. JANOCKO, D. W. CAPONE II, N. J. ZALUZEC, B. FANDERMEYER, O. F. DE LIMA, M. HONG, J. KWO and S. H. LIOU, *J. Appl. Phys.* **62** (1987) 4821.
7. T. NISHIO, Y. ITOH, F. OGASAWARA, M. SUGANUMA, Y. YAMADA and U. MIZUTANI, *J. Mater. Sci.* **24** (1989) 3228.
8. W. D. MACDONALD, A. J. OTTO, E. J. ZWARTZ, B. A. JUDD and E. BATALLA, in "Processing and Applications of High T_c Superconductors", edited by W. E. Mayo (The Metallurgical Society, Rutgers University, N.J. 1988) p. 227.
9. T. ASELAGE and K. KEEFER, *J. Mater. Res.* **3** (1988) 1279.
10. D. L. KAISER, F. HOLTZBERG, M. F. CHISHOLM and T. K. WORTHINGTON, *J. Crystal Growth* **85** (1987) 593.

Received 17 August 1989
and accepted 19 February 1990